Wasit Journal of Engineering Sciences

Journal homepage: https://ejuow.uowasit.edu.iq

Meta surface Assisted Open radio access networks

Haneen A. Ajeel [1], and Ismail Hburi[1]

Affiliations
[1]Department of Electrical Eng. Wasit University, Iraq.

Correspondence
Haneen A. Ajeel
haneenabdajeel@uowasit.edu.iq

Received
18-April-2024
Revised
4-September-2024
Accepted
5-September-2024

Doi:https://doi.org/10.31185/ejuow.Vol12.Iss4.550

Abstract

The paradigm of the open radio access networks (O-RAN) seeks to carry intelligence and openness (multi-vendors) to the conventional proprietary and closed radio access networks (RAN) schemes and deliver performance enhancement, cost-efficiency, and flexibility, in both the network's operation and deployment. On the other hand, Reconfigurable Intelligent Surfaces (RIS) are suggested for future networks due to their effectiveness in terms of cost and energy consumption. However, due to the fast time-varying feature of the dense wireless systems, it becomes difficult to allow optimal user association and beamforming in terms of signalling overheads and processing in RIS assisted RANs with the limited capacity of the fronthaul. This study aims to balance the trade-off between signaling overhead, computational complexity, and throughput performance in a RIS-assisted O-RAN system. We address the technical challenges of jointly selecting optimal UEs/O-RU pairs and designing beamforming strategies at the O-RU, RIS, and O-DU.From this point, to addressing the designing challenges, this work suggests a simple and potential beamforming strategy in RIS aided O-RAN architecture taking into account the specification of the interfaces between different O-RAN units to split opportunities between the radio and distributing units. In specific, a channel-gain-based selection of UEs/O-RU-RIS pairs joint with duality theory (DT) and transform of quadratic function (TQF) algorithm (namely DT_TQF) is proposed.

Firstly, the non-convex optimization problem is relaxed via duality and transform of quadratic functions, and then an iterative approach is carried out for the active and passive beamformers via a simple alternating optimization approach. This approach can achieve flexibility in the environment of a high-traffic transmission while lowering the interference between radio units and the signalling burden required for beamforming tasks. Numerical simulation results justify the effectiveness of the algorithm for different systems' parameter settings and validate the important of installing RIS. For example, for a certain environment, the performance gain is about 52.9 % in comparison to the classic null-steering/random phase shifter scheme.

Keywords: Open-radio access network (O-RAN); Reconfigurable Intelligent Surfaces (RIS); beamforming; duality theory; user-equipment association; transform of quadratic function.

الخلاصة:

يسعى نموذج شبكات الوصول الراديوي المفتوحة (O-RAN) إلى نقل الذكاء والانفتاح (البائعين المتعددين) إلى مخططات شبكات الوصول الراديوي التقليدية والمغلقة (RAN) وتقديم تحسين الأداء وفعالية التكلفة والمرونة، كل من تشغيل الشبكة ونشرها .ومن ناحية أخرى، يُقترح استخدام الأسطح الذكية القابلة لإعادة التشكيل (RIS) للشبكات المستقبلية نظرًا لفعاليتها من حيث التكلفة واستهلاك الطاقة .ومع ذلك، نظرًا لميزة التغير الزمني السريع للأنظمة اللاسلكية الكثيفة، يصبح من الصعب السماح بالارتباط الأمثل للمستخدم وتكوين الحزم فيما يتعلق بإرسال الإشارات العامة والمعالجة في شبكات RAN المدعومة بـ RIS مع السعة المحدودة للوصلة الأمامية .ولذلك، فإن الهدف من هذه الدراسة هو تحقيق المفاضلة بين التكاليف (الإشارة العامة/التعقيد) وأداء الإنتاجية .بمعنى آخر، تحدد الدراسة تحديات تقنية O-RAN بمساعدة RIS فيما يتعلق بالاختيار المشترك لأزواج معدات المستخدم/(UEs) وحدة الراديو المفتوحة (O-RU) وتصميم تشكيل الحزم في O-RU/ RIS والوحدة الموزعة المفتوحة (O-DU).من هذه النقطة، لمعالجة تحديات التصميم، يقترح هذا العمل استراتيجية بسيطة ومحتملة لتشكيل الحزم في بنية O-RAN بمساعدة RISمع الأخذ في الاعتبار مواصفات الواجهات بين وحدات O-RAN المختلفة لتقسيم الفرص بين وحدات الراديو ووحدات التوزيع .وعلى وجه التحديد، يُقترح اختيار قائم على كسب القناة لأزواج تجهيزات المستعمل O-RU-RIS/المرتبطة بنظرية الازدواجية (DT) وخوارزمية

تحويل الدالة التربيعية) (TQF) أي .(DT_TQF أولاً، تم حل مشكلة التحسين غير المحدبة من خلال ازدواجية وتحويل الدوال التربيعية، ومن ثم يتم تنفيذ نهج تكراري لمشكلات الحزم النشطة والسلبية من خلال نهج تحسين متناوب بسيط .يمكن أن يحقق هذا النهج المرونة في بيئة الإرسال ذات الحركة العالية مع تقليل التداخل بين الوحدات الراديوية وعبء الإشارة المطلوب لمهام تكوين الحزم .نتائج المحاكاة العددية تبرر فعالية الخوارزمية لإعدادات معلمات الأنظمة المختلفة وتؤكد أهمية تثبيت .RIS على سبيل المثال، بالنسبة لبيئة معينة، يبلغ معدل زيادة الأداء حوالي 52.9% مقارنةً بنظام ناقل الحركة التقليدي ذو التوجيه الفارغ/مرحلة عشوائية.

1. INTRODUCTION

The peak traffic needs during the next decade are probable to persist in expanding for wireless networks as a result of the increased number of mobile users' equipment (UE) and their capacity. In this aspect, for the vision of the next-generation communication schemes, distinct air-interface paradigms and networking are the two key concepts [1, 2]. As a result, by 2030, it is predicted that unlimited and everywhere connectivity will be required ubiquitous [3]. The virtual tech., open radio access networks (O-RAN), and software aspects, are among the key networking techniques. Whereas air interfaces e.g., comprise intelligent surfaces, and massive multiple-input multiple-output (m-MIMO) technologies. Provided with a high-gain, energy-efficient, and low-cost meta-surface, Reconfigurable Intelligent Surfaces (RIS) is evolving as an optimistic smart radio strategy for future sixth-generation wireless communication systems. [4, 5]. With a considerable number of low-cost passive segments, these Intelligent Surfaces can directed the electromagnetic incident waves to the required direction with increased gain by modifying the elements' phase-shifting angles [6, 7]. Consequently, the enhancements of the transmit power reduction, channel capacity, wireless coverage, and the reliability of transmission all can be attained through the effective controlling of the propagation channel environment via low energy consumption and cost meta-surface units [8, 9]. A RIS is a single, novel, and potentially transformative physical layer technology that enables a new wireless paradigm compatible with future 6G networks. The RISs can transfer data via several passive elements while intelligently altering the communicated route. The growing demand for larger data rate and faster-speed cellular systems for future networks has created severe challenges regarding power consumption, EE and secrecy rate, among other factors. Therefore, the RIS systems must be well-designed, efficient, and interconnected to reach their maximum potential.

This work studies the user association and beamforming issues in the RIS-based O-RAN architecture, which carries together two consistent air-interface and networking elements beyond the fifth-generation networks (B5G) i.e., O-RAN together with RIS technologies. Introduced by the O-RAN Alliance, the O-RAN paradigm, is a version of C-RAN with a virtualized, interoperable interface, and an open network that qualifies products of multiple vendors to work jointly in the same network [10]. To attain the ever-growing information traffic, one favourable way is to use the joint transmission method i.e., allow multiple O-RUs to serve, coherently, UEs and mitigating the interference. Due to the virtualization capability in separate hardware from software, O-RAN not only qualifies for coordinated processing but also builds new energy-efficient prospects and allows, in real-time (RT), the common resource-allocation (RA) in addition, it allows software-based controlling in the near RT [11]. In order to maximize the throughput of the RIS-based-O-RAN system, it’s important to optimize the beamformer at the O-RUs (active-BF) and at the RIS units (Passive-BF) jointly with the user scheduling task. Nevertheless, the non-convexity of this task (both the objective and constraints) makes the optimal solution very difficult to attain. Therefore, a duality theory and quadratic transformation technique are employed to obtain a sub-optimal solution in an iterative method.

2. LITERATURE REVIEW

For C-RAN architecture, authors in [12], [13] suggested various configurations of beamforming function splits between Remote Radio heads and the central pool where the Remote Radio heads are qualified simply for analog-beamforming only (A-BF). Based on information-theoretic strategy, authors in [14], and [15] suggested a beamforming technique to coincide with the restricted fronthaul capability. The same work is repeated in [16], and [17] but with the usage of a scalar quantization assumption. The physical-layer perspectives of O-RAN architecture have been investigated in previous studies in terms of capacity, power consumption, and some other metrics. In [18], the power budget of the front-haul linkage is analysed in a non-power-efficient way assuming all radio-units (RUs) serve all user-equipment (UEs). In [19], authors suggested an optimization formula for the joint allocation of spectrum and a cloud processing of resources where a set of radio units serve the UEs jointly in a user-centric method of user’s association. In [20] the authors, addresses the optimization of the network sum rate and End-to-end power utilization regarding cloud processing of resources and radio/optical front-haul power consumption. The authors in [21]studied the selection of radio-Unit (RU) for joint transmission with front-haul restrictions whereas the power of cloud-processing is considered as a constant factor. In [22], the Physical layer (radio equipment) power utilization is optimized considering the cloud-processing power cost. As we mentioned earlier, Reconfigurable Intelligent Surface (RIS), on the other hand, has been proposed as a potential tech. for future communication systems for its figure of merit in terms of dropping down power consumption and supporting data-traffic performance by

adjusting, artificially, the wireless channel circumstances [23], [24]. In this regard [25] suggest to merged RIS tech. into other 5G potential strategies including the Non-orthogonal Multiple Access (NOMA) schemes. Authors in [26-28] enforce the RIS concept into terahertz wireless MIMO networks that are powered by Artificial Intelligence. The authors in [29]addresses some key specifications that characterize RIS from current technologies in terms of design constraints. In [30] the authors discuss qualities and opportunities for adjusting the wireless environment to boost the bandwidth efficiency of the radio spectrum, extension of the coverage and energy efficiency. Authors in [31] address the enhancement of spatial capacity density and reducing the RIS-based system energy consumption. Ref. [32] provides conceptual work that addresses the challenges in designing meta-surfaces-assisted mobile networks, for example data transmission in the meta-surfaces-assisted circumstances, and boosting or optimization of the resource allocation strategies. While previous works have focused on either minimizing signaling overhead [33] or maximizing data rate [34] independently, this work proposes a novel algorithm that explicitly considers the trade-off between these two critical factors. Unlike [35], which employs a centralized approach, our algorithm utilizes a distributed strategy to reduce the computational burden on the O-DU. This task can be achieved through the joint selection of user's equipment and the designing of active/passive beamforming (active-BF/passive-BF) at the O-RU and RIS units, respectively. This approach with realistic discrete phase-shifter for the passive-BF can achieve flexibility in the environment of a high-traffic transmission while lowering the interference between radio units and the signalling burden required for beamforming tasks. The following points summarizes the contributions of this work.

- At the start point, this article provides a mathematical framework for the proposed RIS-based Open-RAN system to select a beamformer and UEs association that ensure sup-optimal throughput metric while attain the total transmission power.
- After that, the non-convex optimization problem is relaxed via duality and transform of quadratic functions to separate the coupling of the variables of the joint beamforming design. Then, an iterative approach is carried out for the active and passive beamformers via a simple alternating optimization approach.
- Also, numerical simulations are curried out to justify the effectiveness of the algorithm for different systems' parameter settings and validate the important of installing RIS.

The article is organized as follows:
The introduction is presented in Section 1. Then, Section 2 elaborated the scheme Model and formulation of the System equations for the joint selection of user's equipment and the designing of the active-BF and passive-BF. In Section 3 numerical results were debated. Finally, conclusions remarks for the research is completed in section 5.
Notations:
The Small letter signify scalar variables, while capital letters mean scalar constants. Capital bold letters indicates matrices, while vectors are signified by small and bold letters. tr (.), (.)H specifies the Hermitian (conjugate transpose) and matrixes' trace, respectively.

3. MODEL OF THE SYSTEM AND PROBLEM FORMULATION

This section will address both the Model of the scheme and problem formulation aspects.

3.1 Model of the System

In this work, we suppose a scenario with K single-antenna user equipment (UE) served by a number of R units of Open-RAN Radio-Units (O-RUs) with N antennas each. More specifically, this sub-section clarifies the downlink (DL) analysis throughout a certain coherence block. In the proposed architecture, the kth UE is suggested to be served by multiple interfaced O-RUs and their associated Reconfigurable intelligent surfaces (RISs) cooperatively. Each Radio-Unit (O-RU) is supported by S numbers of RISs, each surface is comprised of N reflective segments and these RIS units are controlled by the Open-RAN Distributed-Unit (O-DU) through wireless or wired fronthaul, As shown in figure.1. The transmission from APs to UEs re handled by TDD method, which includes two stages for each coherence period, i.e., Uplink training phase (UL) and Downlink information dispatch (DL). The direct route to the Kth UE is expressed via a complex matrix of $F_{a,k} \in \mathbb{C}^{M \times K}$, where $h_{r,k} \in \mathbb{C}^{N \times 1}$ signifies the RIS-UE route and channel complex matrix1 $G_{a,r}$ of dimension (MxN) signifies the paths between the O-RUs and the intelligent surfaces. The diagonal matrix, $\Phi_s \in \mathbb{C}^{N \times N}$. is the phase-shifting matrix of the obtained signal at the intelligent surface, such that,

$$\Phi_s = \text{diag}.\{\phi_{s1}, \phi_{s2}, \ldots \phi_{sN}\}, \text{ for all } s \in S, \quad \ldots(1)$$

and the individual elements of the Analog-phase shifter can be expressed as follows,

$$\phi_{sn} = C_{sn} . \exp(j\varphi_{sn}), \quad \ldots(2)$$

where, C_{sn} represents the reflection amplitude, and φ_{sn} denotes the discrete phase-shifts levels, where this study considered a discrete value (a finite number) for the phase shift angles of intelligent surface segments to simplify

the realistic execution. If the b-bits2 are employed to describe the level numbers or precision of the phase-shifting, then the number of these levels will be 2^b. The current study also assumed, for the levels of phase shifter, a uniform quantization in the range of [0;2π] for more simplicity. Finally, the discrete phase shift3 values set of the single RIS element will be as follows [36],

$$\varphi_{sn} \in \left\{0, \frac{\pi}{2^{b-1}}, \dots, (2^b - 1).\frac{\pi}{2^{b-1}}\right\}, \quad \text{for all } s \in S \text{ and } n \in N \dots (3)$$

Theoretically, the elements' amplitude of reflection Ϛsn can be modified for different tasks including CSI acquisition and optimizing the system performance. Nonetheless, basically, it is costly to consider an independent controlling scheme for the reflection amplitude and the phase shifter simultaneously. Consequently, an individual reflecting segment is typically considered to optimize the reflected signal phase shift only for the sake of a simple implementation. At the rth O-RU, the transmitted baseband signal vector for all K users, $x_r = [x_{r1}, x_{r2}, \dots, x_{rk}]$, is represented as follows [37]:

$$x_r = \sum_{k=1}^{K} \alpha_{rk} \, . V_{rk} \, S_k \quad \dots (4)$$

where the symbol Sk represents the data to be sent to the kth UE, (k=1, …. K), V_{rk} is an O-RU beamformer vector (active beamformer) for the kth UE, $V_{rk} \in \mathbb{C}^{M \times K} \; \forall \, m \in M,$ and the binary variable α_{rk} is the association factor $\alpha_{rk} \in \{0, 1\}$4, where O-RUs are scheduled to the serving set (A) of a specified UE in accordance with their channel states, i.e., if the rth O-RU unit is selected to be paired with the kth UE, then α_{rk} is set to one, else it is held to zero [38],

$$\alpha_{rk} = \begin{cases} 1, & \text{if } r^{th} \, O - RU \text{ unit is associated.} \\ 0, & \text{otherwise.} \end{cases} \quad \dots\dots (5)$$

Now, the received signal, according to the scheme model addressed above, at the kth UE can be defined as follows5,

$$y_k = \underbrace{\sum_{r \in |R|} F_{rk}^H \, \alpha_{rk} \, V_{rk} S_k}_{\substack{\text{Direct link} \\ \text{desired signal}}} + \underbrace{\sum_{r \in |R|} \sum_{s \in |S|} H_{sk}^H \Phi_s^H \, \alpha_{rk} \, G_{rs} V_{rk} S_k}_{\substack{\text{Reflected link} \\ \text{desired signal}}} + \underbrace{\sum_{r \in |R|} \sum_{\substack{i \in |K| \\ i \neq k}} F_{rk}^H \alpha_{ri} \, V_{ri} S_i + \sum_{r \in |R|} \sum_{s \in |S|} \sum_{\substack{i \in |K| \\ i \neq k}} H_{sk}^H \Phi_s^H \, \alpha_{ri} \, G_{rs} V_{ri} S_i}_{\text{term of interference}} + \sigma_k^2 \quad \dots (6)$$

and the useful signal comprises both direct (O-RU –UE) path and indirect (O-RU -RIS-UE) paths with cascaded channels.

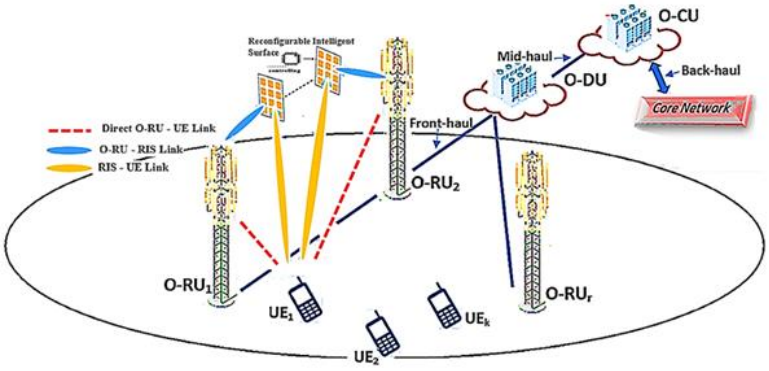

Fig.1 The assumed downlink transmission aided with multiple RISs.

It is remarkable that the most widely used channel model of Saleh-Valenzuela has been assumed [37],

$$g_k = \beta_k^{(0)}\, d\left(\theta_k^{(0)}\right) + \sum_{l\in|L|} \beta_k^{(l)}\, d\left(\theta_k^{(l)}\right) \quad \ldots. \ (7)$$

Where the LoS of the kth UE is signified by $g_k^{LoS} = \beta_k^{(0)}\, d\left(\theta_k^{(0)}\right)$, in which $\beta_k^{(0)}$ indicates the complex gain and $d\left(\theta_k^{(0)}\right)$ denotes the spatial direction. Also, the L total number of Non-LoS rays,

$g_k^{NLoS} = \sum_{l=1}^{L} \beta_k^{(l)}\, d\left(\theta_k^{(l)}\right)$ for $1 \le l \le L$ is the lth NLoS components of the kth UE. Now, the received signal yk in (6) can be expressed as,

$$y_k = \sum_{r\in|R|} \sum_{s\in|S|} \sum_{i\in|K|} \left(\alpha_{ri}\, F_{rk}^H + H_k^H \Phi_s^H\, \alpha_{ri}\, G_s\right) V_i S_{ri} + \sigma_k^2 \quad \ldots (8)$$

where the symbols $G_s, \Phi,$ and V_k are as follows; the first symbol is ${G_s}^T = [{g_{1s}}^T, {g_{2s}}^T, \ldots\ {g_{Rs}}^T]$, the second is, $\text{diag.}\{\Phi_1, \Phi_2, \ldots \Phi_S\}$, and ${V_k}^T = [{v_{1k}}^T, {v_{2k}}^T, \ldots\ {v_{Rk}}^T]$. Besides, for the sake of simplifying the notation and the mathematical expression, let us utilize the symbol Q_k to signify the overall cascading channel as follows,

$$Q_k^H = F_k^H + \sum_{s\in|S|} H_k^H \Phi_s^H G_s \quad \ldots (9)$$

It's worth bearing in mind that, based on the time-division duplex protocol, the channel reciprocity approach can be employed to evaluate the DL channel through the acquired UL-pilot sequences from the UEs. By creating the RIS-assisted linkage (as depicted in fig. 1) through the cascaded channel, to acquire the CSI one can employ compressive sensing (CS) according to the sparse features of the cascaded channel or the formal MSE technique. Hence, the received signal at kth user is expressed as follows,

$$y_k = \sum_{i\in|K|} Q_k^H\, \alpha_{ri}\, V_i S + \sigma_{k_i}^2 \quad \ldots (10)$$

Similarly, the SINR of this UE for the above scheme can be signified as follow,

$$\Gamma_k(\Phi, V) = \frac{\left\|\sum_{r\in|R|} \sum_{s\in|S|} \left(F_{rk}^H + H_k^H \Phi_s^H G_s\right) V_i\right\|_2^2}{I_{O-RUs} + I_{RISs} + \sigma_k^2}, \quad \ldots (12)$$

where the term, $\left\|\sum_{r\in|R|} \sum_{s\in|S|} \left(F_{rk}^H + H_k^H \Phi_s^H G_s\right) V_i\right\|_2^2$ corresponds to the useful channel gain and the terms of the denominator of this equation can be represented as follows,

$$I_{O-RUs} + I_{RISs} = \sum_{\substack{i\in|K| \\ i\neq k}} \left\| \sum_{r\in|R|} \sum_{s\in|S|} \left(F_{rk}^H + H_k^H \Phi_s^H G_s\right) V_i \right\|_2^2 \quad \ldots (13)$$

Equation (12) can be written in terms of the equivalent channel as follows,

$$\Gamma_k(\Phi, V) = \frac{V_k^H Q_k Q_k^H V_k}{\sum_{\substack{i\in|K| \\ i\neq k}} V_i^H Q_k Q_k^H V_i + z_k}, \quad \ldots (14)$$

where $z_k \sim CN(0, \sigma_k^2)$ denotes the Additive White Gaussian Noise (AWGN). Ultimately, data throughput (nats/sec/Hz) per channel use [37], [39] is shown as,

$$R_t = \sum_{k\in|K|} \ln\left(1 + \Gamma_k(\Phi, V)\right), \quad \ldots (15)$$

and the power-allocation optimizing formula can be expressed as follows6,

Ƥ0

$$\max_{\Phi,V} \sum_{k\in|K|} \ln\left(1+\Gamma_k(\Phi,V)\right), \quad \dots(16)$$

s.t

$$C_1;\ \phi_{sn} = C_{sn}.\exp(j\varphi_{sn}), \quad \dots(16a)$$

$$C_2;\ \varphi_{sn} \in \left\{0, \frac{\pi}{2^{b-1}}, \dots, \left(2^b-1\right).\frac{\pi}{2^{b-1}}\right\}, \quad \text{for all } s\in S \text{ and } n\in N \dots(16b)$$

$$C_3: \qquad \text{trac.}\left(V_k V_k^H\right) \le P_{max} \qquad \dots(16c)$$

where Pmax signifies the O-RU's maximum acceptable transmitting power. The limitation of phase shift for the reflecting element is detailed in the restriction of equation (16a). Retained to the constraints in equations (16a) and (16b), the optimization problem addressed in equation (16) is a significantly complex problem task. For the objective function of the problem Ƥ0, it is crucial to decouple the optimization variables to attain an attractable problem. In this study, To obtain a solution for problem (16), we devise a distributed approach to release the heavy burden of the fronthaul signalling overhead where only adjacent O-RUs are needed to exchange little reports with each other.

3.2 Beamforming Design Algorithm

Next, we are going to exploit the dual formulation strategy that was submitted in reference [5] to decompose the logarithm term employing the theory of duality (DT). Therefore, the log-term in equation (3) will be addressed with aid of another auxiliary variable μ_k^1, where $\mu_k^1 \in \mathbb{R}^{n\times k}$ and return number of $|R|$ trackable subproblems. As a result, the optimizing problem Ƥ0 in (16) is identical to the following expression7,

Ƥ1:

$$\max_{\Phi,V,\mu} \sum_{k\in|K|} \ln(1+\mu_k^1) - \sum_{\substack{r\in|A|\\ s\in|S|}} \sum_{k\in|K|} \mu_k^1 + \sum_{\substack{r\in|A|\\ s\in|S|}} \sum_{k\in|K|} (1+\mu_k^1).\frac{\Gamma_k(\Phi,V)}{1+\Gamma_k(\Phi,V)} \quad \dots(17)$$

s.t.:

$$C_1; \qquad \phi_{sn} = C_{sn}.\exp(j\varphi_{sn}), \qquad \dots(17a)$$

$$C_2;\ \varphi_{sn} \in \left\{0,\ \pi.(2^{b-1}), \dots, \pi.\left(2^b-1\right).(2^{b-1})\right\}, \quad \text{for all } n\in N \text{ and } s\in S \dots(17b)$$

$$C_3: \qquad \text{trac.}\left(V_k V_k^H\right) \le P_{Max} \qquad \dots(17c)$$

here, $\mu^1 = [\mu_1^1, \mu_2^1, \dots \mu_K^1]^T$. It is clear that in Ƥ1, equation (17a) is the constraint on ϕ_{sn}, and equation (17c) is the constraint on V_k. For the sake of disconnecting the optimization variables' coupling of the problem Ƥ1, the current study is motivated to use the transform of a quadratic function (TQF). It is worth bearing in mind that the standard Dinkelbach approach is hard to engage as a result of the dimensional completeness of such a fractional formula. Thus, further auxiliary variables are utilized (μ3 and μ2) to resolve the O-RU beamform vector task V and passive beamforming Φ (reflected beamforming from RIS) in an iteratively converged strategy. This solution applied the alternating optimization (AO) approach by keeping the RIS's reflection beamform vector Φ at a fixed value to perform the V optimizing and then keeping V at a fixed value to perform the Φ optimizing in a consequence procedure till attain convergence8. After that, the optimizing task Ƥ0 can be performed for V, Φ,and μ at a small cost of computational complexity, of the flowchart that gives the details of beamform vectors (active/passive-BF) devise algorithm-I. In particular, sub-problems are required to be evaluated, subsequently, to update or renew the values of the variables μ_k^{1*} based on V*, Φ*, and zero value of the differentiation, $\frac{\partial \mathcal{P}1}{\partial \mu_k^1} = 0$, which leads to closed form of $\mu_k^{1*} = \Gamma_k$. As a result, for the new values of $\Phi^*$and μ_k^{1*} the task in equation (17) will be as follows,

Ƥ2:

$$\max_{V,\Phi} \sum_{k\in|K|} (1 + \mu_k^1).\frac{\Gamma_k(\Phi,V)}{1+\Gamma_k(\Phi,V)} \quad \dots(18)$$

s.t

$$C_1; \quad \phi_{sn} = C_{sn}.\exp(j\varphi_{sn}),$$

$$C_2; \quad \varphi_{sn} \in \{0, \pi.(2^{b-1}), \dots, \pi.(2^b-1).(2^{b-1})\}, \text{ for all } n \in N \text{ and } s \in S$$

$$C_3: \quad \text{trac.}(V_k V_k^H) \le P_{max}$$

Hence, the logarithmic optimization NP-hard problem has been recast to a much easier problem in (18) where the optimization of V, and Φ, can be done alternatively. After that, leverage the tactic employed in [40] using the transform of a quadratic function (TQF) and introducing a new auxiliary variable $\mu_k^2 \in \mathbb{C}$ K. The problem in equation (18) with a fixed Φ and A can be defined in a lower sophisticated format with a single restriction condition,

Ƥ 2:

$$\underset{V}{\text{maximize}} \quad \sum_k 2\sqrt{1+\mu_k^{1*}}\ \text{Rel.}\{\mu_k^2 Q_k^H V_k^H\} - \sum_k \mu_k^{2H}.(\sum_{\substack{i\in|K|\\ i\neq k}} V_i^H Q_k Q_k^H V_i + 1)$$

s.t.:

$$\text{trac.}(V_k V_k^H) \le P_{max} \quad \dots(19)$$

With the symbol Rel. {.} signifies the real part of what is inside the bracket (the complex number).

O-RU's active-BF optimizing

The following sub-problem is considered to optimize V_k and μ_k^2 in equation (19) alternatively9. At first point, by keeping V at a fixed value to determine μ_k^{2*} with zero value of the differentiation, $\frac{\partial P2}{\partial \mu_k^2} = 0$, here the optimal values μ_k^2 can be updated as in equation 20 [32],

$$\mu_k^{2*} = \frac{\sqrt{1+\mu_k^{1*}}.Q_k^H V_i}{\sum_{\substack{i\in|K|\\ i\neq k}} V_i^H Q_k Q_k^H V_i + z_k} \quad \dots(20)$$

Next, by keeping μ_k^2 at a fixed value to perform optimization of the vector V* in the formula of eq.19, and to lower the task sophisticated, another objective task Ƥ 3 is updated from Ƥ 2 as in equation 21,

Ƥ3:

$$\max_V \ -V^H E\ V + 2\ \text{Rel.}\{U^H V\} - Y \quad \dots(21)$$

s.t.:

$$V^H X\ V \le P_{max}$$

Where:

$$E = I_k \otimes \sum_k Q_k\ \mu_k^2\ \mu_k^{2H}\ Q_k^H$$

$$Y = \sum_k \mu_k^{2H}\ z_k\ \mu_k^2$$

$$U^T = [u_1, u_2, \dots . u_k]$$

$$u_k = \mu_k^{2H}\ Q_k^H\ V_k$$

$$X = I_k \otimes E$$

The symbol ⊗ signifies the Kronecker product which produces block matrices. As a result of existed Semi-Definite Programming restraints (SDP) in equation (21), the updating of the O-RUs' active-BF can be performed through any suitable package (e.g., the CVX package which is a disciplined convex program tool).

RIS Passive-BF Optimizing

Now, the role is to fulfil $\mu 3k \in \mathbb{C}$ K updating after keeping V^* , A, and μ_k^{1*} all fixed. For this case, the optimizing task will be as follows: Ƥ4;

$$\max_{\Phi} \sum_{k} (1 - \mu_k^{1*}).\Gamma_k(\Phi, V^*) \quad \dots (22)$$

s. t. ;

$$\Phi_{sn} \in \{0, \pi.2^{b-1}, \dots, (2^b - 1).\pi.2^{b-1}\}, \text{ for all } s \in S \text{ and } n \in N$$

In addition, this condition is still hard to obtain accurately, thus, the current study choices the transform of a quadratic function (TQF) and introduces another variable μ_k^3 [40]. Accordingly, The task in equation (22) will be as follows,

Ƥ5;

$$\max_{\Phi} \sum_{k} 2\sqrt{1 + \mu_k^{1*}}\ \text{Rel.}\{\mu_k^{3H}.W_k\} - \mu_k^{3H}(\sum_{\substack{i\in|K| \\ i\neq k}} W_i W_i^H + z_k)\,\mu_k^3$$

s.t.;

$\Phi_{sn} \in \{0, \pi.(2^{b-1}), \dots, \pi.(2^b - 1).(2^{b-1})\}$, for all $n \in N$ and $s \in S$.

where,

$$W_k = \sum_{r\in|R|} \left(F_{rk}^H + H_k \Phi^H G_r\right).V_k \quad \dots (23)$$

Now, in a technique similar to the previous strategy, sub-problem Ƥ5 in equation (23) will be reduced into a couple of simpler tasks as below, when Φ is fixed, the subproblem to find optimal W_k is simplified to the SE optimization of the traditional multiuser MIMO problem. This issue has been considered much in the publications, and one notable way to acquire the answer is the MMSE approach using an iterative algorithm10 to update the variable. First, find μ_k^{3*} for fixed Φ via $\frac{\partial P5}{\partial \mu 3K} = 0$,

$$\mu_k^{3*} = \frac{\sqrt{1 + \mu^{1*}}.W_k(\Phi)^*}{\sum_{\substack{i\in|K| \\ i\neq k}} W_i(\Phi)^* + z_k} \quad \dots (24)$$

Second, Ƥ5 will be simplified into Ƥ5 as shown below, Ƥ6;

$\max_{\Phi}. \quad -\Phi^H ß\, \Phi + 2\,\text{Re}\{\Phi^H b\} - a \quad \dots (25)$

s.t.; For simplicity's sake and decreasing the cost of computations, an iterative algorithm is employed to resolve the values of $\boldsymbol{\Phi}$ and $\mathbf{W}_k$.

$$\Phi_{r,n} \in \{0, \pi.(2^{b-1}), \dots, \pi.(2^b - 1).(2^{b-1})\}, \text{ for all } n \in N \text{ and } s \in S$$

given that,(25a)

$$ß = \sum_r \sum_k \text{diagnal}\{\mu_k^{3H} H_k^H\} G_{rs} V_k (G_{rs} V_k)^H$$

$$b = \sum_r \sum_k \sqrt{1 + \mu_k^{1*}}\ \text{diag.}\{\mu_k^{3H} H_k^H\} G_a V_k - \sum_r \sum_k \mu_k^{3H} F_{rk}^H V_k^* (\mu_k^{3H} F_{rk}^H V_k^*)$$

$$a = \sum_k \& \left|\sum_r \mu_k^{3H} F_{rk}^H V_k\right| 2 + \sum_k \mu_k^{3H} z_k \mu_k^3 - 2\sum_k \sqrt{1 + \mu_k^{1*}}\ \text{Rel.}\left\{\sum_r \mu_k^{3H} F_{rk}^H V_k\right\}$$

Now, due to the SDP constraints of this problem (17), the updating of the intelligent surface's passive-BF can be performed employing any disciplined convex optimization tool. Table I shows the outline of the proposed algorithm, where, according to the norm or gain of the corresponding channels $\|Q_k\|_2$, the first stage is to set all the O-RUs' units in a descending order, and the candidate set of O- RUs with high gain of the channel is to be allocated to serve the kth user. The association procedure depends on the coefficients of the UEs' effective channel. If we keep Φ fixed then these coefficients can be determined and consequently sorted in a descending ordering where kth UE is just attached to O-RUs which have the higher effective channel gains.

Table 1: The Pseudo-code for the proposed algorithm.

Start Algorithm-I:

1. Initialize the set of parameters for the system including: user's number |K|, total transmit power P_t, iteration index: $t = 0$, direct O-RU-UE link F, O-RU-RIS link G, and RIS-UE link H.
2. Initial random variable: V*, Φ*
3. Update iteration index t = t+1

1st STAGE; select Candidate set of O-RUs for the kth UE:

4. Set number of best O-RUs set |A| for the kth UE, Compute user's effective channel norms: $M = \{\|Q_k\|_2, \ \forall \ r \in |R|\}$,
5. Sort O-RUs set according to channel gain $\|Q_k\|_2$ in a descending order: $\Psi = \text{sort}$ (M, 'descent'), Sort users according to channel norms.
6. For all $m \in \Psi$;
7. If; the gain $\|Q_k\|_2 < \Theta_{th}$, Then: $O - RU_m \in |A|$. End If

2nd STAGE; O-RUs Digital Beamforming

8. Employ V*, Φ*, and $\frac{\partial P1}{\partial \mu_k^1} = 0$, then update μ_k^{1*} such that, $\mu_k^{1*} = \Gamma_k$
9. Employ μ_k^{1*}, Φ*, and $\frac{\partial P2}{\partial \mu_k^2} = 0$ then update μ2* from (11), $\mu_k^{2*} = \frac{\sqrt{1+\mu_k^{1*}} Q_k^H V_i}{\sum_{\substack{i \in |K| \\ i \neq k}} V_i^H Q_k Q_k^H V_i + z_k}$
10. Evaluate V* from eq. (12), Ƥ3: $\max_V \ -V^H E V + 2 \ \text{Rel.}\{U^H V\} - Y$

IRS-Reflection analog Beamforming;

11. Evaluate μ3* using eq. (21), $\mu_k^{3*} = \frac{\sqrt{1+\mu^{1*}} W(\Phi)^*}{\sum_{i \in k} W_{k,i}(\Phi)^* w_{k,i}(\Phi)^* + z_k}$
12. Evaluate Φ* from eq. (22), Ƥ6: Max $(\Phi) \ -\Phi^H ß \Phi + \text{Rel.}\{2\Phi^H b\} - \alpha$
13. Calculate Rt using eq. (15), Ƥ0: $\max_{\Phi,V} \ \sum_{k \in |K|} \ln(1 + \Gamma_k)$
14. Check convergence; go to step (3) if not.
15. Return, A, V, Φ, and Rt.

As depicted in table I, the first step is to initialize a set of parameters, i.e., AP-RIS path and iteration index. Following that, random variables for active beamforming (transmit beamforming) V*, passive beamforming (reflect beamforming) Φ* are set. Then using these variables (V*,Φ*) and $\frac{\partial P1}{\partial \mu_k^1} = 0$ lead to closed form for $\mu_k^{1*}=\Gamma_k$ to update of μ1*. Following by computing μ_k^{2*} from equation (11) as follows by using μ1*, Φ*, $\mu_k^{2*} = \frac{\sqrt{1+\mu_k^{1*}} Q_k^H V_i}{\sum_{\substack{i \in |K| \\ i \neq k}} V_i^H Q_k Q_k^H V_i + z_k}$ ... (26).

Next, the formula has been transformed into a concave-convex algorithm, which can solve the convex maximization problem V via the CVX tool according to equation (12), which is expressed as:

$\max_V \ -VH\,E\,V + 2 \ \text{Rel.}\{UH\,V\} - Z$ ... (27).

The next stage in the flowchart is to update from equation (28) as displayed:

$\mu_k^{3*} = \frac{\sqrt{1+\mu^{1*}} W_k(\Phi)^*}{\sum_{\substack{i \in |K| \\ i \neq k}} W_i(\Phi)^* + z_k}$ ... (28).

Then computes Φ* by solving the equation (27) as;

$\max_\Phi \ -\Phi^H ß \Phi + 2 \ \text{Rel.}\{\Phi^H b\} - a$ ... (29)

via CVX toolbox, followed by calculating Rt (throughput) until convergence.

Next, we will discuss our suggested joint user association and beamforming technique in terms of computational complexity. For the first stage, i.e., selecting the candidate set of O-RUs for the kth UE, there is linear complexity with the order of magnitude, [41], where, R is the number of best O-RUs set, and K is the number of the deployed users. For the O-RUs Digital Beamforming, Updating the auxiliary variable u1 has a complex of around O{ (K+1)KR M2} in each iteration of this algorithm, while updating auxiliary variable u2 needs near O{K2M2R} floating point operations, and updating the digital beamforming Vk requires of O{(RM+3)+KRM2]} floating point operations. The significant complexity comes from updating the Analog Beamforming which has a complexity of the order, O{(R+3K+2KR)[R3K3M2]}. Therefore, the total complexity of the proposed algorithm is on the order of about, O{(R+3K+2KR)[R3K3M2]+(RM+3)+KRM2]+K2M2R}.

4. SIMULATION RESULTS AND DISCUSSION

The previous section discussed the research methods employed in this study. In this part, using MATLAB® 2019b, the numerical results of the suggested intelligent surfaces-based O-RAN system with corresponding discussion will be delivered for different scenarios.

4.1Simulation Parameters

The current study considered that the arrival/departure angles are distributed randomly over the range from 0 rad up to 2π rad. In addition, realistic implementation of intelligent surfaces required limited levels of discrete weights for phase shifting. In the current study for the reference system to compare the performance with, a benchmark scheme is utilized with Null-steering digital beamforming and Random Analog phase shifter. Null-steering (a.k.a Zero-forcing) is a strategy of linear spatial processing of the signal in the multi-user multiple input multiple output antenna communication system (MU-MIMO) where the aim is to null the interference induced by user multiplexing using pseudo-inverse of the channel matrix as a special pre-coder with the following closed-form formula, $V = (G^H G)^{-1}$. On the other hand, since $e^{j\theta}$, $\theta \in \mathbb{R}$. is a periodic function of a 2π period, therefore both [−π, π) and [0, 2π) can be employed for the phase shifter initializing. Consequently, each reflecting element in the RIS surface is assigned with the phase shift which is initialized by selecting a random phase value from the interval [θ, θ+2π) and y is any uniform distributed random real number. Simulation parameters have been set as shown in Table. The path loss as a function of the LOS distance between the TX and the RX is estimated in accordance with the Standard Linear model,

Path-loss (d) [dB] = αPL + βPL.10. log10(d) + ξ, …(30)

where d [in meters] is the TX / RX distance, αPL is the floating intercept least square fits of the measured distances and β is the slope least square fits of the measured distances, and ξ is a lognormal shadowing r.v with variance of σ^2_{Ln} .

Table 2: Parameters' setting for the simulation environments.

Parameter	Setting
Channel model	3-dimension mm-Wave Saleh-Valenzuela model [4]
Path loss estimation	Standard Linear model [42, 43]
Path loss floating intercept least square	αPL [LoS, NLoS] = [70.0, 61.4] dB
Path loss slope least square	βPL[LoS, NLoS] = [2.9, 2.0] dB
lognormal shadowing STD-deviation	σ_{Ln}[LoS, NLoS] = [72.0, 5.8] dB
Maximum Power Transmission	P_t = 32 dBm
Transmission frequency	28 GHz
Noise power	$n^2 = -95$ dBm
Phase-shifters quantize digits (D)	[1-9] bits and infinite resolution Phase-shifter
RIS elements' Number	[10 -128]
O-RU antenna number	16 elements
Number of user-equipment UE	[2, 3] users
Number of O-RU	3 Units
Benchmark algorithm for comparison	Null-steering11 digital beamforming and a Random Analog phase shifter [14]

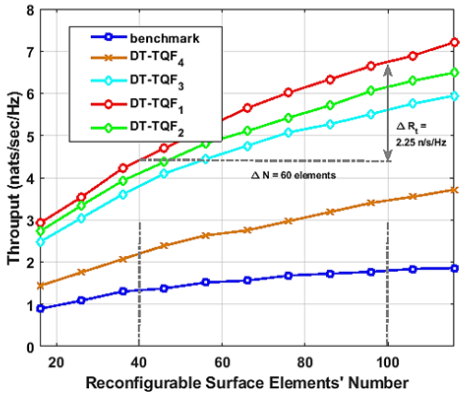

Fig.2 The Impact of the Reconfigurable Surface Elements' number on the System throughput performance.

Figure 2 illustrates the system throughput versus Reconfigurable Surface Elements' number while preserving the total power of the O-RUs at 15 dBm and the number of the UEs at 2-user. The simulation compares the performance of the benchmark scheme with the proposed algorithm which is carried out for four different cases of DT-TQF (1 through 4) for various levels of phase-shifter (PS) resolution (continuous-PS, 3-bit PS,2-bit PS, and 1-bit PS, respectively). It is obvious that when Elements' number is increased, the throughput of the scheme with the proposed algorithm is enhanced as a result of the aggregation of the reflected signals by the Reconfigurable Surface growths the level of the overall signal. For instance, for continuous-PS scenario, growing the surface elements from 40 to 100 elements can increase the UE rate by nearly 33.6 % (4.5 to 6.75 nats/sec/Hz). In addition, the 3-bit PS scenario (DT-TQF2) performs very close to the perfect resolution (DT-TQF1) case. Also, if we compare between proposed scheme (3-bit PS resolution) and the traditional scheme (null-steering with random PS), for N=40 elements, the performance gain is about 52.9 %. Consequently, the proposed approach can achieve an acceptable performance trade-off for cost burden in practical systems.

Figure. 3 illustrates the effects of increasing the transmission power on the system throughput for different numbers of UEs' cases (increases exponentially). In addition, different PS-resolution are tested, cases (1, 3, and 5) are for 2-bit discrete PS, while cases (2,4, and 6) are for perfect or continuous PS. As shown in the figure, for the case of 2-bit discrete PS, for example, increasing the power from 25 dBm up to 33 dBm can enhance the throughput by almost 35.0 %. Again, there is a very small gap between the two cases of 2-bit discrete PS and the continuous PS, therefore, the proposed algorithm is appropriate for practical application with low-cost PSs.

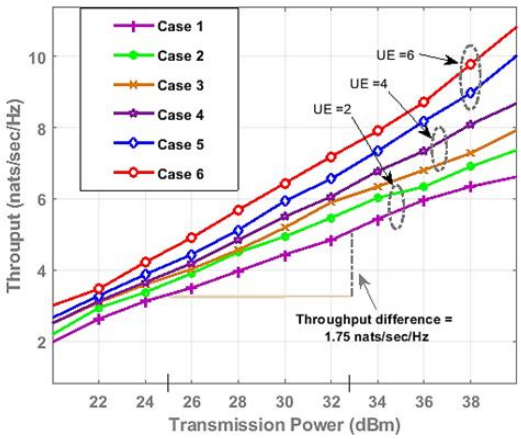

Fig .3 System throughput performance versus the power of transmission.

Regarding the number of iterations, Figure 4, shows the convergence rate for various scenarios. More specifically, different numbers of UEs and RIS elements' Number are tested and compared. In this figure, the (users-RIS elements) pair for scenarios DT-TQF (1 through 4) is as follows, (UEs, N) = (4, 40), (4, 30), (3, 30), and (2, 20), respectively. As depicted in this figure, the iteration burden of increasing the number of UEs from 2-user up to 4-user is about 4-iteration.

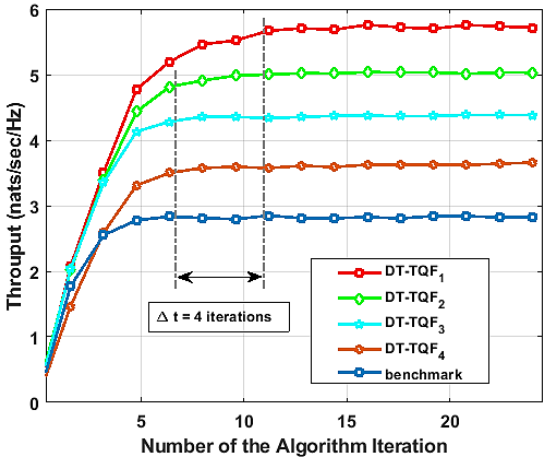

Fig. **Error! No text of specified style in document.** System throughput performance versus the number of the algorithm iteration (convergence performance).

Figure 5, displays the impact of increasing the PS resolution on the system performance where 3-different numbers of UEs (2, 3, and 4-user) are tested for three cases of discrete PS scenarios (2, 3, and 4-bit). Specifically, this figure displays the gap or drawback in the performance of the discrete PS cases in comparison with the perfect full-resolution case. For example, in the case of two UEs, the gap is about 0.054 nats/sec/Hz.

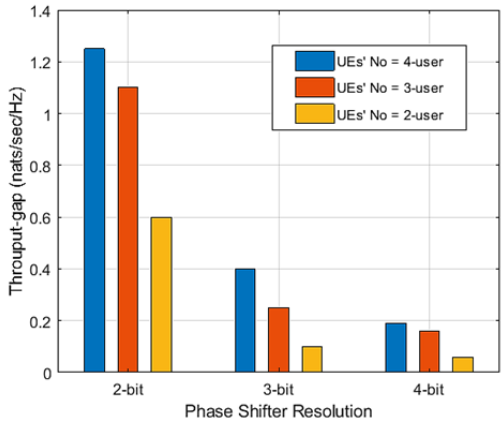

Fig. 5 Average symbol error probability with versus RIS elements.

In the same aspect, Figure 6 shows in more detail the effects of the PS resolution on the system throughput performance. More specifically, different numbers of UEs are compared for two cases (3-bit discrete PS (coloured curves) and the continuous PS (dashed grey curves)). Scenarios (1, 2, and 3) are for numbers of UEs = (2, 3, and 4, respectively). At Phase shifter resolution of b = 4 bits, almost both the discrete and continuous PSs have the same performance. while for the case of b= 3-bit the performance drawback between the discrete and continuous PSs for scenarios 1, 2, and 3 are about 1.4, 2.8, and 3.3 nats/sec/Hz.

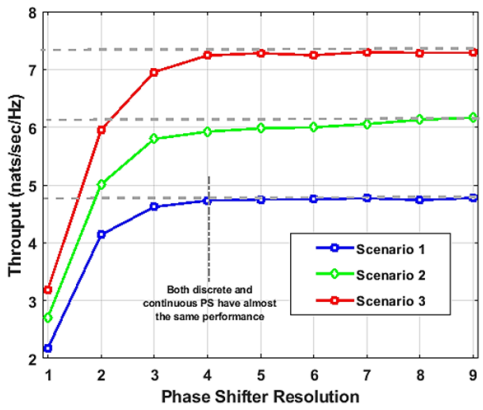

Fig. 6 The Impact of the resolution of the Analog Phase Shifter on the System throughput performance.

5. CONCLUSIONS

To accomplish a trade-off between the signaling overhead and the throughput performance in RIS-based Open-RANs an alternating iterative approach is suggested to jointly select user's equipment and design the active-BF/passive-BF with a practical discrete phase-shifter. While the proposed algorithm shows promising performance gains, practical implementation challenges remain. One key challenge is the accurate estimation of the channel state information (CSI) for the RIS-assisted links. Imperfect CSI can significantly degrade the performance of the algorithm. Potential solutions include employing robust beamforming techniques [44]or developing more efficient CSI acquisition methods [45]. Further research is needed to address these challenges and realize the full potential of RIS-assisted O-RANs. Obtained results validate the effectiveness of the algorithm for different systems' parameter settings and show the important of employing of the RIS technique.

REFERENCES

1. Jiang, W., et al., *The road towards 6G: A comprehensive survey.* 2021. **2**: p. 334-366.
2. Hburi, I.S. and H.F. Khazaal. *Joint RRH selection and power allocation forEnergy-efficient C-RAN systems*. in *2018 Al-Mansour International Conference on New Trends in Computing, Communication, and Information Technology (NTCCIT)*. 2018. IEEE.
3. Han, C., Y. Wu, and Z.J.I.T.U. Chen, *Network 2030 a blueprint of technology, applications and market drivers towards the year 2030 and beyond.* 2018.
4. Hburi, I., et al. *MISO-NOMA Enabled mm-Wave: Sustainable Energy Paradigm for Large Scale Antenna Systems*. in *2021 International Conference on Advanced Computer Applications (ACA)*. 2021. IEEE.
5. Hua, M., et al., *Intelligent reflecting surface-aided joint processing coordinated multipoint transmission.* 2020. **69**(3): p. 1650-1665.
6. Al-Shaeli, I., et al., *Reconfigurable intelligent surface passive beamforming enhancement using unsupervised learning.* 2023. **13**(1): p. 493-501.
7. Hasan Fahad KHazaal, Ahmed Magdy, Iryna Svyd, IVAN OBOD, *A Dumbbell Shape Reconfigurable Intelligent Surface for mm-wave 5G Application.* International Journal of Intelligent Engineering and Systems, 2024. **17**(6): p. 569-582.
8. Imoize, A.L., et al., *A review of energy efficiency and power control schemes in ultra-dense cell-free massive MIMO systems for sustainable 6G wireless communication.* 2022. **14**(17): p. 11100.
9. Salim, H., et al., *Reconfigurable Intelligent Surfaces Between the Reality and Imagination.* Wasit Journal of Computer and Mathematics Science, 2024. **3**(2): p. 42-50.
10. Polese, M., et al., *Understanding O-RAN: Architecture, interfaces, algorithms, security, and research challenges.* 2023. **25**(2): p. 1376-1411.
11. Malandrino, F., et al. *Performance and EMF exposure trade-offs in human-centric cell-free networks*. in *2022 20th International Symposium on Modeling and Optimization in Mobile, Ad hoc, and Wireless Networks (WiOpt)*. 2022. IEEE.
12. Park, S.-H., et al., *Fronthaul compression for cloud radio access networks: Signal processing advances inspired by network information theory.* 2014. **31**(6): p. 69-79.
13. Peng, M., et al., *Fronthaul-constrained cloud radio access networks: Insights and challenges.* 2015. **22**(2): p. 152-160.
14. Kim, J., et al. *Joint design of digital and analog processing for downlink C-RAN with large-scale antenna arrays*. in *2017 IEEE 18th International Workshop on Signal Processing Advances in Wireless Communications (SPAWC)*. 2017. IEEE.
15. Kang, J., et al., *Layered downlink precoding for C-RAN systems with full dimensional MIMO.* 2016. **66**(3): p. 2170-2182.
16. Liu, L. and R.J.I.T.o.S.P. Zhang, *Optimized uplink transmission in multi-antenna C-RAN with spatial compression and forward.* 2015. **63**(19): p. 5083-5095.
17. Liu, L., S. Bi, and R.J.I.T.o.C. Zhang, *Joint power control and fronthaul rate allocation for throughput maximization in OFDMA-based cloud radio access network.* 2015. **63**(11): p. 4097-4110.
18. Agheli, P., M.J. Emadi, and H.J.a.p.a. Beyranvand, *Designing cost-and energy-efficient cell-free massive MIMO network with fiber and FSO fronthaul links.* 2020.
19. Wang, X., et al., *Virtualized cloud radio access network for 5G transport.* 2017. **55**(9): p. 202-209.
20. Demir, Ö.T., et al., *Cell-free massive MIMO in O-RAN: Energy-aware joint orchestration of cloud, fronthaul, and radio resources.* 2024.
21. Pan, C., et al., *Joint precoding and RRH selection for user-centric green MIMO C-RAN.* 2017. **16**(5): p. 2891-2906.
22. Ha, V.N. and L.B. Le. *Computation capacity constrained joint transmission design for c-rans*. in *2016 IEEE Wireless Communications and Networking Conference*. 2016. IEEE.
23. Taha, A., M. Alrabeiah, and A.J.I.a. Alkhateeb, *Enabling large intelligent surfaces with compressive sensing and deep learning.* 2021. **9**: p. 44304-44321.
24. Renzo, M.D., et al., *Smart radio environments empowered by reconfigurable AI meta-surfaces: An idea whose time has come.* 2019. **2019**(1): p. 1-20.
25. Keti, F., et al., *Spectral and energy efficiencies maximization in downlink NOMA systems.* 2022. **11**(3): p. 1449-1459.
26. Mishra, D.P., et al., *Compact MIMO antenna using dual-band for fifth-generation mobile communication system.* 2021. **24**(2): p. 921-929.
27. Elbir, A.M., et al., *Deep channel learning for large intelligent surfaces aided mm-wave massive MIMO systems.* 2020. **9**(9): p. 1447-1451.

28. Rashag, H.F. and M.H.J.I.J.o.A.i.A.S.I. Ali, *Optimization of transmission signal by artificial intelligent.* 2019. **2252**(8814): p. 8814.
29. Huang, C., et al., *Holographic MIMO surfaces for 6G wireless networks: Opportunities, challenges, and trends.* 2020. **27**(5): p. 118-125.
30. Dardari, D.J.I.J.o.S.A.i.C., *Communicating with large intelligent surfaces: Fundamental limits and models.* 2020. **38**(11): p. 2526-2537.
31. Huang, C., et al., *Reconfigurable intelligent surfaces for energy efficiency in wireless communication.* 2019. **18**(8): p. 4157-4170.
32. ElMossallamy, M.A., et al., *Reconfigurable intelligent surfaces for wireless communications: Principles, challenges, and opportunities.* 2020. **6**(3): p. 990-1002.
33. Sokal, B., et al., *Reducing the control overhead of intelligent reconfigurable surfaces via a tensor-based low-rank factorization approach.* 2023. **22**(10): p. 6578-6593.
34. Praia, J., et al., *Phase shift optimization algorithm for achievable rate maximization in reconfigurable intelligent surface-assisted THz communications.* 2021. **11**(1): p. 18.
35. Alexandropoulos, G.C., et al. *Phase configuration learning in wireless networks with multiple reconfigurable intelligent surfaces*. in *2020 IEEE Globecom Workshops (GC Wkshps*. 2020. IEEE.
36. Wang, P., et al., *Intelligent reflecting surface-assisted millimeter wave communications: Joint active and passive precoding design.* 2020. **69**(12): p. 14960-14973.
37. Hburi, I., et al. *Sub-array hybrid beamforming for sustainable largescale mmWave-MIMO communications*. in *2021 International Conference on Advanced Computer Applications (ACA)*. 2021. IEEE.
38. HUbri, I., F.J.I.J.o.E.E. Hasan, and C. Science, *An Efficient Two-Stage User Association Scheme for Green C-RAN Systems.* 2019. **16**(2): p. 793-802.
39. Baqer, I.S. *A practical weighted sum rate maximisation for multi-stream cellular MIMO systems*. in *2018 International Conference on Engineering Technology and their Applications (IICETA)*. 2018. IEEE.
40. Shen, K. and W.J.I.T.o.S.P. Yu, *Fractional programming for communication systems—Part I: Power control and beamforming.* 2018. **66**(10): p. 2616-2630.
41. Singh, S.K., R. Singh, and B. Kumbhani. *The evolution of radio access network towards open-RAN: Challenges and opportunities*. in *2020 IEEE Wireless Communications and Networking Conference Workshops (WCNCW)*. 2020. IEEE.
42. Błaszczyszyn, B. and M.J.P.o.W. Karray, Paderborn, *Linear-regression estimation of the propagation-loss parameters using mobiles' measurements in wireless cellular network.* 2012.
43. Zakeri, H., R.S. Shirazi, and G.J.a.p.a. Moradi, *An Accurate Model to Estimate 5G Propagation Path Loss for the Indoor Environment.* 2023.
44. Gao, H., et al., *Robust beamforming for reconfigurable intelligent surface-assisted multi-cell downlink transmissions.* 2024.
45. Gao, S., et al., *Deep multi-stage CSI acquisition for reconfigurable intelligent surface aided MIMO systems.* 2021. **25**(6): p. 2024-2028.